in Proc. IEEE ICASSP 2011
Prague, Czech Republic, May 2011, pp. 3484–3487

DIRECTION-RESOLVED ESTIMATION OF MULTIPATH PARAMETERS FOR UWB CHANNELS: A PARTIALLY COLLAPSED GIBBS SAMPLER METHOD

Georg Kail[1], *Klaus Witrisal*[2], *and Franz Hlawatsch*[1]

[1]Institute of Telecommunications, Vienna University of Technology, Austria; {gkail, fhlawats}@nt.tuwien.ac.at
[2]SPSC Lab, Graz University of Technology, Austria; witrisal@tugraz.at

ABSTRACT

We propose a Monte Carlo method for determining the parameters of multipath components (MPCs) for ultra-wideband channels. A *partially collapsed Gibbs sampler* is used for jointly estimating the number, times-of-arrival, angles-of-arrival, and amplitudes of the MPCs as well as the sounding pulse from signals received by a 2D antenna array. Our system model accounts for propagation delays between the receive antennas. Temporal-angular sparsity of the detected MPCs is ensured by a 2D minimum distance constraint. Numerical results for synthetic and real signals demonstrate the excellent performance and fast convergence of our method.

***Index Terms*—** Ultra-wideband channel, channel estimation, multipath component, partially collapsed Gibbs sampler.

1. INTRODUCTION

The high temporal resolution of ultra-wideband (UWB) technology allows for precise positioning and ranging. Recent work suggests to exploit reflected multipath components (MPCs) for enhancing UWB-based indoor positioning [1,2]. This requires estimation of the times-of-arrival, angles-of-arrival, and amplitudes of the MPCs. Algorithms proposed for this problem include successive cancellation techniques like the Sensor-CLEAN algorithm [3] and extensions [4]. Furthermore, the SAGE algorithm has been applied to estimation of UWB channel parameters in the frequency domain [5] and to estimation of wideband channel parameters in the time domain [6]. However, the SAGE-based methods rely on a system model that is narrowband in that the times-of-arrival at all receive antennas are assumed to be equal, which is not valid for bandwidths close to or larger than the ratio of propagation velocity and array dimension. It has been shown in [7] that the performance of the SAGE-based methods can be significantly improved by enforcing a minimum temporal distance between detected MPCs.

Here, we propose a *partially collapsed Gibbs sampler* (PCGS) [8, 9] for joint estimation of the MPC parameters (number, times-of-arrival, angles-of-arrival, and amplitudes) and of the pulse shape. The PCGS is a Markov chain Monte Carlo method [10] that is well suited for joint estimation of a large number of possibly strongly dependent parameters. It has previously been applied to Bernoulli-Gaussian sequences with a minimum distance constraint [9]. As a difference from [7], we use a minimum temporal distance constraint that is restricted to an angular interval around MPCs; this constitutes a more realistic 2D constraint. Furthermore, our system model is better suited to UWB signals because it accounts for propagation delays between the receive antennas. Finally, the pulse shape and the number of MPCs (model order) are not assumed to be known at the receiver but are estimated along with the MPC parameters.

This paper is organized as follows. The system model and the stochastic model are presented in Sections 2 and 3, respectively. Section 4 describes the detection-estimation method. Numerical results are presented in Section 5.

This work was supported by the Austrian Science Fund (FWF) under Grants S10603 and S10604 within the National Research Network SISE.

2. SYSTEM MODEL

A UWB pulse is transmitted around center frequency c/λ, where c is the speed of light and λ is the wavelength. The transmitter-scatterer-receiver configuration is approximately static, so that Doppler shifts can be neglected. The signal propagates in 2D space and is received by a 2D array of M receive antennas with antenna responses $f_m(\phi)$ and 2D locations $\mathbf{r}_m$, for $m = 1, \ldots, M$. Each of the M received signals consists of L MPCs. The lth MPC is characterized by its amplitude α_l, time-of-arrival τ_l, and angle-of-arrival ϕ_l, with $l \in \{1, \ldots, L\}$. All MPCs have a common pulse shape $h(t)$, which is unknown at the receiver due to distortions caused by antenna detuning. Note that we do not account for individual distortions of the pulse shape along the different propagation paths.

The baseband signal received by the mth antenna is given by

$$y_m(t) \;=\; \sum_{l=1}^{L} \alpha_l \, h\big(t - \tau_l + \eta_m(\phi_l)\big) \, c_m(\phi_l) \;+\; n_m(t)\,, \qquad (1)$$

with $\eta_m(\phi) \triangleq \mathbf{e}^{\mathrm{T}}(\phi)\,\mathbf{r}_m/c$ and $c_m(\phi) \triangleq \exp\big(j2\pi\,\mathbf{e}^{\mathrm{T}}(\phi)\,\mathbf{r}_m/\lambda\big) \cdot f_m(\phi)$. Here, $n_m(t)$ is noise, $\mathbf{e}(\phi)$ is the unit-length vector with angle ϕ, and the superscript $^{\mathrm{T}}$ denotes transposition. Arranging the M factors $c_m(\phi)$ into a vector yields the steering vector of the antenna array for angle ϕ. A common simplification, justified in narrowband settings, is to neglect the different $\eta_m(\phi)$ in (1). However, this will not be done here in view of the shortness of UWB pulses.

For a discrete-time representation, we set $t = kT$, $\tau_l = k_l T$, and $\phi_l = q_l \cdot 2\pi/Q$, with $k, k_l, q_l \in \mathbb{Z}$ and suitable sampling periods T and $2\pi/Q$, where $Q \in \mathbb{N}$. If T is sufficiently small, we can replace $\eta_m(\phi)$ by its discretized version $\eta_{m,q} \triangleq \mathrm{round}\big\{\frac{1}{T}\,\eta_m(q \cdot 2\pi/Q)\big\}$. We then obtain from (1) the discrete-time signal model

$$y_m[k] \;=\; \sum_{l=1}^{L} \alpha_l \, h[k - k_l + \eta_{m,q_l}] \, c_m[q_l] \;+\; n_m[k]\,,$$

with $y_m[k] \triangleq y_m(kT)$, $h[k] \triangleq h(kT)$, $c_m[q_l] \triangleq c_m(q_l \cdot 2\pi/Q)$, and $n_m[k] \triangleq n_m(kT)$. Hereafter, we assume that $y_m[k]$ is observed for $k = 1, \ldots, K$. Since the model order L is unknown, it will be convenient to reformulate α_l using a 2D time-angle indexing:

$$\alpha_{k,q} \triangleq \begin{cases} \alpha_l, & (k,q) = (k_l, q_l), \;\; l = 1, \ldots, L \\ 0, & \text{else}, \end{cases} \qquad (2)$$

for $k = 1, \ldots, K$ and $q = 1, \ldots, Q$. Then, our model reads

$$y_m[k] \;=\; \sum_{k'=1}^{K} \sum_{q=1}^{Q} \alpha_{k',q}\, h[k-k'+\eta_{m,q}]\, c_m[q] \;+\; n_m[k]\,. \qquad (3)$$

This can be expressed as

$$\mathbf{y} \;=\; \mathbf{H}\boldsymbol{\alpha} + \mathbf{n}\,, \qquad (4)$$

where the $(m+(k-1)M)$th entry of $\mathbf{y} \in \mathbb{C}^{MK}$ equals $y_m[k]$ (and similarly for $\mathbf{n}$); the $(q+(k'-1)Q)$th entry of $\boldsymbol{\alpha} \in \mathbb{C}^{KQ}$ equals $\alpha_{k',q}$; and the entry of $\mathbf{H} \in \mathbb{C}^{MK \times KQ}$ in the $(m+(k-1)M)$th row and $(q+(k'-1)Q)$th column equals $h[k-k'+\eta_{m,q}]\, c_m[q]$.

Our goal is to estimate $\boldsymbol{\alpha}$ from $\mathbf{y}$, without knowledge of $\mathbf{H}$. According to (2), the length-KQ vector $\boldsymbol{\alpha}$ is L-sparse (i.e., only L of its entries are nonzero), with some unknown L. Typically, $L \ll KQ$. Enforcing sparsity in the estimate $\hat{\boldsymbol{\alpha}}$ avoids spurious entries that are caused by overfitting due to modeling errors and noise. Following [7, 9], this can be achieved by enforcing a minimum temporal distance between detected MPCs (i.e., nonzero entries of $\hat{\boldsymbol{\alpha}}$). Here, we modify this minimum-distance constraint in that we do not constrain the temporal distance of two MPCs if their angular distance is sufficiently large. Our constraint thus reads as follows: for any two nonzero entries $\hat{\alpha}_{k,q}$ and $\hat{\alpha}_{k',q'}$, either $|k-k'| \geq d_1$ or $\min_{i\in\{-1,0,1\}} |q-q'+iQ| \geq d_2$ or both, where d_1 and d_2 are, respectively, the temporal and angular minimum distances. Thus, for any fixed k and q, the set $\{\hat{\alpha}_{k+\Delta k,\,(q+\Delta q) \bmod Q}\}$ with $0 \leq \Delta k \leq d_1-1$ and $0 \leq \Delta q \leq d_2-1$ contains at most one nonzero element.

In Section 4, we will also use the following alternative system description that shows the relation between the sequences $h[k]$ and $y_m[k]$ more explicitly than (3), (4):

$$y_m[k] \;=\; \sum_{k'=-N}^{N} \sum_{l=1}^{L} \alpha_l\, c_m[q_l]\, \delta[k-k'-k_l+\eta_{m,q_l}]\, h[k'] \;+\; n_m[k]\,,$$

where we assumed $h[k]=0$ for $|k|>N$, with some $N>0$. This can be expressed as

$$\mathbf{y} \;=\; \mathbf{A}\mathbf{h} + \mathbf{n}\,, \qquad (5)$$

where the k'th entry of $\mathbf{h} \in \mathbb{C}^{2N+1}$ equals $h[k'-N-1]$ and the entry of $\mathbf{A} \in \mathbb{C}^{MK\times(2N+1)}$ in the $(m+(k-1)M)$th row and k'th column equals $\sum_{l=1}^{L} \alpha_l\, c_m[q_l]\, \delta[k-(k'-N-1)-k_l+\eta_{m,q_l}]$.

3. STOCHASTIC MODEL

Priors. The Bayesian methodology requires prior distributions for all quantities to be estimated or detected. To define the prior distribution of the $\alpha_{k,q}$, we introduce the auxiliary binary indicator variables

$$b_{k,q} \;\triangleq\; \begin{cases} 0\,, & \alpha_{k,q}=0 \\ 1\,, & \alpha_{k,q}\neq 0\,, \end{cases} \qquad k=1,\ldots,K;\; q=1,\ldots,Q\,.$$

Each nonzero $b_{k,q}$ (i.e., each $b_{k,q}=1$) indicates the time k and angle q of an MPC. Note that $\sum_{k=1}^{K}\sum_{q=1}^{Q} b_{k,q} = L$. We will represent the $b_{k,q}$'s as a vector $\mathbf{b} \in \{0,1\}^{KQ}$ that is defined analogously to $\boldsymbol{\alpha}$. Since $\mathbf{b}$ is a function of $\boldsymbol{\alpha}$, the prior of $\boldsymbol{\alpha}$ can be decomposed as

$$p(\boldsymbol{\alpha}) \;=\; p\big(\boldsymbol{\alpha}, \mathbf{b}(\boldsymbol{\alpha})\big) \;=\; p\big(\boldsymbol{\alpha}|\mathbf{b}(\boldsymbol{\alpha})\big)\, p\big(\mathbf{b}(\boldsymbol{\alpha})\big)\,.$$

We model the conditional prior $p(\boldsymbol{\alpha}|\mathbf{b})$ as

$$p(\boldsymbol{\alpha}|\mathbf{b}) \;=\; \prod_{k=1}^{K}\prod_{q=1}^{Q} p(\alpha_{k,q}|b_{k,q})\,,$$

with (note that $b_{k,q}=0$ implies $\alpha_{k,q}=0$)

$$p(\alpha_{k,q}|b_{k,q}=0) = \delta(\alpha_{k,q})\,, \;\; p(\alpha_{k,q}|b_{k,q}=1) = \mathcal{CN}(\alpha_{k,q}; 0, \sigma_k^2)\,.$$

Here, $\sigma_k^2 = \sigma_\alpha^2 \gamma^k$ with fixed hyperparameters σ_α^2 and $\gamma \in (0,1]$; the factor γ^k (with γ chosen close to 1) models the increase of the path loss with the path length. Because $b_{k,q}$ indicates whether the associated $\alpha_{k,q}$ is zero or nonzero, we can incorporate our miminum-distance constraint in the prior of $\mathbf{b}$ by setting

$$p(\mathbf{b}) \;\propto\; \mathcal{B}(\mathbf{b};\pi_1)\, \mathrm{I}_{\mathcal{M}}(\mathbf{b})\,. \qquad (6)$$

Here, $\mathcal{B}(\mathbf{b};\pi_1) \triangleq \pi_1^L (1-\pi_1)^{KQ-L}$, with $L = L(\mathbf{b}) = \sum_{k=1}^{K}\sum_{q=1}^{Q} b_{k,q}$, is the product of KQ independent Bernoulli distributions with "1-probability" π_1 (a fixed hyperparameter), and $\mathrm{I}_{\mathcal{M}}(\mathbf{b})$ is the indicator function of the set $\mathcal{M}$ of binary sequences $\mathbf{b}$ satisfying the miminum-distance constraint.

Because of the minimum-distance constraint, the indicators $b_{k,q}$ are not statistically independent, since a nonzero indicator causes the surrounding indicators to be zero. More specifically, for each index pair $(k,q) \in \{1,\ldots,K-d_1+1\} \times \{1,\ldots,Q\}$, let us define the rectangular region $\mathcal{J}(k,q) \triangleq \{k,\ldots,k+d_1-1\} \times \{q,(q+1) \bmod Q,\ldots,(q+d_2-1) \bmod Q\}$. Furthermore, let $\mathbf{b}_{\mathcal{J}(k,q)} \in \{0,1\}^{d_1 d_2}$ denote the subvector of $\mathbf{b}$ containing all $b_{k',q'}$ with $(k',q') \in \mathcal{J}(k,q)$, and let $\mathbf{b}_{\sim\mathcal{J}(k,q)} \in \{0,1\}^{KQ-d_1 d_2}$ denote the complementary subvector of $\mathbf{b}$. Note that the subvectors $\mathbf{b}_{\mathcal{J}(k,q)}$ are partly overlapping. Each of them contains $d_1 d_2$ indicators $b_{k',q'}$, of which at most one is nonzero. Indeed, any $\mathbf{b}$ for which one or more subvectors $\mathbf{b}_{\mathcal{J}(k,q)}$ contain more than one nonzero entry is assigned a prior probability of zero via the factor $\mathrm{I}_{\mathcal{M}}(\mathbf{b})$ in (6).

The entries of the pulse-shape vector $\mathbf{h} \in \mathbb{C}^{2N+1}$ will be assumed statistically independent, zero-mean, and complex Gaussian, i.e., $p(\mathbf{h}) = \mathcal{CN}(\mathbf{h};\mathbf{0},\mathbf{D}_{\boldsymbol{\sigma}_\mathbf{h}})$, where $\mathbf{D}_{\boldsymbol{\sigma}_\mathbf{h}} \triangleq \mathrm{diag}(\boldsymbol{\sigma}_\mathbf{h})$ with a fixed vector of variances $\boldsymbol{\sigma}_\mathbf{h}$. By assigning small values to the early and late entries of $\boldsymbol{\sigma}_\mathbf{h}$ and larger values to the middle entries, we obtain pulse shapes $h[k]$ that tend to be centered around $k=0$.

The entries of the noise vector $\mathbf{n}$ are modeled as independent and identically distributed, zero-mean, and complex Gaussian, i.e., $p(\mathbf{n}) = \mathcal{CN}(\mathbf{n};\mathbf{0},\sigma_n^2\mathbf{I}_{KM})$, where $\mathbf{I}_{KM}$ denotes the identity matrix of size $KM \times KM$. The noise variance σ_n^2 is a random hyperparameter that will be estimated jointly with the model parameters using a hierarchical Bayesian model. For its prior, we use an inverse gamma distribution $\mathcal{IG}(\sigma_n^2;\xi,\zeta)$ as suggested in [11], with fixed hyperparameters ξ and ζ. The values of the fixed hyperparameters σ_α^2, γ, π_1, $\boldsymbol{\sigma}_\mathbf{h}$, ξ, and ζ are assumed to be known.

Joint posterior. Bayesian detection/estimation of $\mathbf{b}$, $\boldsymbol{\alpha}$, $\mathbf{h}$, and σ_n^2 is based on the joint posterior distribution, which is given by

$$p(\boldsymbol{\alpha},\mathbf{b},\mathbf{h},\sigma_n^2|\mathbf{y}) \;\propto\; p(\mathbf{y}|\boldsymbol{\alpha},\mathbf{h},\sigma_n^2)\, p(\boldsymbol{\alpha}|\mathbf{b})\, p(\mathbf{b})\, p(\mathbf{h})\, p(\sigma_n^2)\,, \quad (7)$$

with the likelihood $p(\mathbf{y}|\boldsymbol{\alpha},\mathbf{h},\sigma_n^2) = \mathcal{CN}(\mathbf{y};\mathbf{H}\boldsymbol{\alpha},\sigma_n^2\mathbf{I}_{KM})$ (see (4)). Note that $p(\boldsymbol{\alpha}|\mathbf{b})$, $p(\mathbf{h})$, and $p(\sigma_n^2)$ are conjugate priors [10] for this likelihood.

4. DETECTION AND ESTIMATION

To ensure sparsity of our estimate of $\boldsymbol{\alpha}$, we first detect $\mathbf{b}$ using a MAP detector and then estimate each $\alpha_{k,q}$ given the corresponding detected indicator $\hat{b}_{k,q}$ (if it is nonzero). For this second step, as well as for estimating $\mathbf{h}$ and σ_n^2, we use an MMSE estimator. These detectors and estimators require various marginals of $p(\boldsymbol{\alpha},\mathbf{b},\mathbf{h},\sigma_n^2|\mathbf{y})$ in (7), which cannot be calculated in closed form. We therefore employ a Markov chain Monte Carlo (MCMC) sampling method [10] to generate a sample $\mathcal{S}$ of I realizations $\big\{(\boldsymbol{\alpha},\mathbf{b},\mathbf{h},\sigma_n^2)^{(i)}\big\}_{i=1,\ldots,I}$ drawn from $p(\boldsymbol{\alpha},\mathbf{b},\mathbf{h},\sigma_n^2|\mathbf{y})$. The detection/estimation is then based on $\mathcal{S}$. The task of marginalization now simply amounts to ignoring the irrelevant components of the realizations $(\boldsymbol{\alpha},\mathbf{b},\mathbf{h},\sigma_n^2)^{(i)}$.

Estimators and detectors. Sample-based MMSE estimation of $\mathbf{h}$ and σ_n^2 amounts to an averaging of the respective realizations, i.e.,

$$\hat{\mathbf{h}} = \frac{1}{I}\sum_{i=1}^{I}\mathbf{h}^{(i)}, \quad \widehat{\sigma_n^2} = \frac{1}{I}\sum_{i=1}^{I}(\sigma_n^2)^{(i)}.$$

For sample-based MAP detection of $\mathbf{b}$, we define a sample-based approximation $p_{\mathcal{S}}(b_{k,q})$ to the posterior probability $p(b_{k,q}|\mathbf{y})$ of $b_{k,q} \in \{0,1\}$ as the number of realizations $(\boldsymbol{\alpha}, \mathbf{b}, \mathbf{h}, \sigma_n^2)^{(i)}$ that contain the respective value of $b_{k,q}$, normalized by I. The sample-based componentwise MAP detector of $\mathbf{b}$ is then given by

$$\hat{b}_{k,q} = \arg\max_{b_{k,q}\in\{0,1\}} p_{\mathcal{S}}(b_{k,q}), \quad k = 1,\ldots,K.$$

For a discussion of limitations of this componentwise detector and a description of possible alternatives, see [12].

For sample-based MMSE estimation of $\alpha_{k,q}$ given $\hat{b}_{k,q}$, we partition the set of sample indices $\{1,\ldots,I\}$ into two complementary subsets $\mathcal{I}_{k,q}(0)$ and $\mathcal{I}_{k,q}(1)$ containing all indices i for which $b_{k,q}^{(i)} = 0$ and $b_{k,q}^{(i)} = 1$, respectively. Then, $\alpha_{k,q}$ is estimated as

$$\hat{\alpha}_{k,q} = \frac{1}{|\mathcal{I}_{k,q}(\hat{b}_{k,q})|}\sum_{i\in\mathcal{I}_{k,q}(\hat{b}_{k,q})}\alpha_{k,q}^{(i)}.$$

Here, $|\mathcal{I}|$ denotes the number of elements of $\mathcal{I}$. Note that $\hat{\alpha}_{k,q} = 0$ if $\hat{b}_{k,q} = 0$, because all realizations $\alpha_{k,q}^{(i)}$ with $i \in \mathcal{I}_{k,q}(0)$ are zero.

Besides the dominant MPCs that are to be estimated, UWB signals typically contain numerous small MPCs that result from diffuse scattering and are not desired in the estimate. We can eliminate them by a thresholding, i.e., by defining our final estimate as $\hat{\bar{\alpha}}_{k,q} = \hat{\alpha}_{k,q}$ for $|\hat{\alpha}_{k,q}| > \rho_k$ and $\hat{\bar{\alpha}}_{k,q} = 0$ else, where $\rho_k \triangleq \rho_0\sqrt{\gamma^k}$ exhibits the same temporal decay as $\sigma_k = \sigma_\alpha\sqrt{\gamma^k}$ in the prior of $\alpha_{k,q}$.

MCMC sampling algorithm. The simplest algorithm for generating a sample $\{(\boldsymbol{\alpha}, \mathbf{b}, \mathbf{h}, \sigma_n^2)^{(i)}\}_{i=1,\ldots,I}$ from $p(\boldsymbol{\alpha}, \mathbf{b}, \mathbf{h}, \sigma_n^2|\mathbf{y})$ is the Gibbs sampler [10], which can be described generically as follows. Let $\boldsymbol{\vartheta}$ be a vector of J parameters (which may themselves be vectors), and let $\boldsymbol{\vartheta}_{\sim j}$ denote $\boldsymbol{\vartheta}$ without the jth parameter (vector) $\boldsymbol{\vartheta}_j$. To obtain a sample from $p(\boldsymbol{\vartheta})$, realizations of each $\boldsymbol{\vartheta}_j$ are iteratively generated from $p(\boldsymbol{\vartheta}_j|\boldsymbol{\vartheta}_{\sim j})$, i.e., from the distribution of $\boldsymbol{\vartheta}_j$ conditioned on the most recently sampled values of all other parameters. Under some mild conditions, this strategy converges to the target distribution $p(\boldsymbol{\vartheta})$ regardless of the initialization. After convergence, J such sampling substeps (for all $j \in \{1,\ldots,J\}$) produce a new realization of $\boldsymbol{\vartheta}$ drawn from $p(\boldsymbol{\vartheta})$.

A weakness of the Gibbs sampler is that dependencies between the $\boldsymbol{\vartheta}_j$ tend to result in slow convergence [11]. In particular, the dependencies due to the minimum-distance-constraint factor $\mathrm{I}_{\mathcal{M}}(\mathbf{b})$ in $p(\boldsymbol{\alpha}, \mathbf{b}, \mathbf{h}, \sigma_n^2|\mathbf{y})$ (see (6), (7)) may violate the conditions for convergence. The problem of strongly dependent parameters is usually solved by sampling these parameters jointly. However, in practice, $\mathbf{b}$ cannot be sampled jointly due to the large number of hypotheses (2^{KQ}). Also, the minimum-distance constraint does not introduce a block structure with strong dependencies only within each block. Instead, the constraint causes each $b_{k,q}$ to be strongly dependent on its individual neighborhood. This means that the subvectors of $\mathbf{b}$ within which the $b_{k,q}$ should be sampled jointly are not disjoint, which violates the Gibbs sampler concept.

This limitation is overcome by the *partially collapsed Gibbs sampler* (PCGS) [8, 9]. The PCGS allows us to sample the parameters $b_{k,q}$ and $\alpha_{k,q}$ within each region $\mathcal{J}(k,q)$ jointly, even though these regions strongly overlap. Some parameters are sampled in more than one substep. Convergence is still guaranteed, and, for strongly dependent parameters, it is much faster than that of the Gibbs sampler. One iteration of the proposed PCGS-based sampling algorithm consists of the following substeps.

- For each $(k,q) \in \{1,\ldots,K-d_1+1\} \times \{1,\ldots,Q\}$,
  - sample $\mathbf{b}_{\mathcal{J}(k,q)}$ from $p\big(\mathbf{b}_{\mathcal{J}(k,q)}\big|\mathbf{b}_{\sim\mathcal{J}(k,q)}, \boldsymbol{\alpha}_{\sim\mathcal{J}(k,q)}, \mathbf{h}, \sigma_n^2, \mathbf{y}\big)$;
  - sample $\boldsymbol{\alpha}_{\mathcal{J}(k,q)}$ from $p\big(\boldsymbol{\alpha}_{\mathcal{J}(k,q)}\big|\mathbf{b}, \boldsymbol{\alpha}_{\sim\mathcal{J}(k,q)}, \mathbf{h}, \sigma_n^2, \mathbf{y}\big)$.
- Sample $\mathbf{h}$ from $p(\mathbf{h}|\mathbf{b}, \boldsymbol{\alpha}, \sigma_n^2, \mathbf{y})$.
- Sample σ_n^2 from $p(\sigma_n^2|\mathbf{b}, \boldsymbol{\alpha}, \mathbf{h}, \mathbf{y})$.

The validity of the first two substeps is not obvious, since the sampling distributions are not conditionals with respect to the full joint posterior $p(\boldsymbol{\alpha}, \mathbf{b}, \mathbf{h}, \sigma_n^2|\mathbf{y})$. However, it can be verified that the two substeps taken together amount to jointly sampling $\mathbf{b}_{\mathcal{J}(k,q)}$ and $\boldsymbol{\alpha}_{\mathcal{J}(k,q)}$ from $p\big(\mathbf{b}_{\mathcal{J}(k,q)}, \boldsymbol{\alpha}_{\mathcal{J}(k,q)}\big|\mathbf{b}_{\sim\mathcal{J}(k,q)}, \boldsymbol{\alpha}_{\sim\mathcal{J}(k,q)}, \mathbf{h}, \sigma_n^2, \mathbf{y}\big)$, which is a conditional with respect to $p(\boldsymbol{\alpha}, \mathbf{b}, \mathbf{h}, \sigma_n^2|\mathbf{y})$.

Sampling distributions. Using our statistical assumptions of Section 3, the sampling distribution for $\mathbf{b}_{\mathcal{J}(k,q)}$ can be shown to be

$$p\big(\mathbf{b}_{\mathcal{J}(k,q)}\big|\mathbf{b}_{\sim\mathcal{J}(k,q)}, \boldsymbol{\alpha}_{\sim\mathcal{J}(k,q)}, \mathbf{h}, \sigma_n^2, \mathbf{y}\big) \propto \begin{cases} (1-\pi_1)/\pi_1\,, & \mathbf{b}_{\mathcal{J}(k,q)} = \mathbf{0} \\ (\sigma^2/\sigma_{\hat{k}}^2)\, e^{|\mu|^2/\sigma^2}\mathrm{I}_{\mathcal{M}}(\mathbf{b})\,, & \text{else}\,, \end{cases} \tag{8}$$

with

$$\mu = \frac{\sigma^2}{\sigma_n^2}\mathbf{h}_{\hat{k},\hat{q}}^{\mathrm{H}}\big(\mathbf{y} - \mathbf{H}_{\sim\mathcal{J}(k,q)}\boldsymbol{\alpha}_{\sim\mathcal{J}(k,q)}\big)$$

$$\sigma^2 = \left(\frac{\|\mathbf{h}_{\hat{k},\hat{q}}\|^2}{\sigma_n^2} + \frac{1}{\sigma_{\hat{k}}^2}\right)^{-1}.$$

Here, $\mathbf{h}_{k,q}$ is the column of $\mathbf{H}$ corresponding to $\alpha_{k,q}$ and $\mathbf{H}_{\sim\mathcal{J}(k,q)}$ comprises the columns of $\mathbf{H}$ corresponding to $\boldsymbol{\alpha}_{\sim\mathcal{J}(k,q)}$. The superscript $^{\mathrm{H}}$ denotes conjugate transposition. In the case where $\mathbf{b}_{\mathcal{J}(k,q)} \neq \mathbf{0}$, $(\hat{k},\hat{q})$ denotes the position of the nonzero entry. Note that $\mathbf{H}$ is constructed using the most recently sampled realization of $\mathbf{h}$, i.e., it is updated in each iteration. Sampling from (8) requires that we evaluate that probability for all hypotheses. Since it involves the prior $p(\mathbf{b})$, we can exploit the minimum-distance constraint: the fact that each region $\mathcal{J}(k,q)$ contains at most one nonzero element drastically reduces the number of hypotheses from $2^{d_1 d_2}$ to $d_1 d_2 + 1$ (one hypothesis with no 1 and $d_1 d_2$ hypotheses with one 1; recall that each $\mathcal{J}(k,q)$ contains $d_1 d_2$ indicators).

Like $\mathbf{b}_{\mathcal{J}(k,q)}$, $\boldsymbol{\alpha}_{\mathcal{J}(k,q)}$ contains at most one nonzero entry. Since the current realization of $\mathbf{b}_{\mathcal{J}(k,q)}$ is included in the condition of the sampling distribution $p\big(\boldsymbol{\alpha}_{\mathcal{J}(k,q)}\big|\mathbf{b}, \boldsymbol{\alpha}_{\sim\mathcal{J}(k,q)}, \mathbf{h}, \sigma_n^2, \mathbf{y}\big)$, we already know whether it contains a nonzero entry. If it does not, the realization of $\boldsymbol{\alpha}_{\mathcal{J}(k,q)}$ is determined to be zero. If it does, then sampling $\boldsymbol{\alpha}_{\mathcal{J}(k,q)}$ reduces to sampling the corresponding $\alpha_{\hat{k},\hat{q}}$ from $p\big(\alpha_{\hat{k},\hat{q}}\big|\mathbf{b}, \boldsymbol{\alpha}_{\sim\mathcal{J}(k,q)}, \mathbf{h}, \sigma_n^2, \mathbf{y}\big)$. This latter sampling distribution can be shown to be given by $\mathcal{CN}\big(\alpha_{\hat{k},\hat{q}}; \mu, \sigma^2\big)$, with μ and σ^2 as above.

The sampling distribution for $\mathbf{h}$ can be shown to be given by $p(\mathbf{h}|\mathbf{b}, \boldsymbol{\alpha}, \sigma_n^2, \mathbf{y}) = \mathcal{CN}(\mathbf{h}; \boldsymbol{\mu}_{\mathbf{h}}, \boldsymbol{\Sigma}_{\mathbf{h}})$, with (cf. (5))

$$\boldsymbol{\mu}_{\mathbf{h}} = \frac{1}{\sigma_n^2}\boldsymbol{\Sigma}_{\mathbf{h}}\mathbf{A}^{\mathrm{H}}\mathbf{y}\,, \quad \boldsymbol{\Sigma}_{\mathbf{h}} = \left(\frac{1}{\sigma_n^2}\mathbf{A}^{\mathrm{H}}\mathbf{A} + \mathbf{D}_{\boldsymbol{\sigma}_{\mathbf{h}}}^{-1}\right)^{-1}.$$

The matrix $\mathbf{A}$ is constructed using the most recently sampled realization of $\boldsymbol{\alpha}$, i.e., it is updated in each iteration.

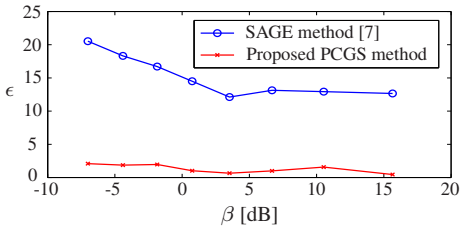

Fig. 1. MPC detection from synthetic UWB signals: ϵ versus β.

Finally, using the inverse gamma prior $\mathcal{IG}(\sigma_n^2;\xi,\zeta)$ of σ_n^2, the sampling distribution for σ_n^2 can be shown to be

$$p(\sigma_n^2|\mathbf{b},\boldsymbol{\alpha},\mathbf{h},\mathbf{y}) = \mathcal{IG}\big(\sigma_n^2;\xi+KQ\,,\zeta+\|\mathbf{y}-\mathbf{H}\boldsymbol{\alpha}\|^2\big)\,.$$

5. NUMERICAL RESULTS

We generated 800 realizations of $\mathbf{y}$ from parameters randomly drawn from the priors specified in Section 3, using $K=80$, $Q=64$, $N=10$, $d_1=d_2=5$, $\sigma_\alpha^2=8\cdot10^{-9}$, $\gamma=0.984$, $\xi=1.25\cdot10^9$, $\zeta=0.5$, $\lambda=5.45$cm, and $T=1.6\cdot10^{-10}$s. The pulse shape $h(t)$ is a root-raised-cosine pulse with baseband bandwidth 2GHz. The entries of $\boldsymbol{\sigma}_\mathbf{h}$ are chosen large in the center and small towards the first and last entries. The receiver uses a 10×10 antenna array with spacings of 2cm. We assume that $f_m(\phi)\equiv1$. MPCs with $|\alpha_{k,q}|>\rho_0\sqrt{\gamma^k}$ are considered as dominant MPCs, whereas the others are considered as undesired diffuse MPCs; their amplitudes are denoted by $\boldsymbol{\alpha}_{\text{dom}}$ and $\boldsymbol{\alpha}_{\text{diff}}$, respectively (with $\boldsymbol{\alpha}_{\text{dom}}+\boldsymbol{\alpha}_{\text{diff}}=\boldsymbol{\alpha}$). To achieve different values of $\beta\triangleq\mathrm{E}\{\|\boldsymbol{\alpha}_{\text{dom}}\|^2\}/\mathrm{E}\{\|\boldsymbol{\alpha}_{\text{diff}}\|^2\}$, ρ_0 is varied between $0.5\,\sigma_\alpha$ and $1.8\,\sigma_\alpha$ and π_1 is varied between 0.0018 and 0.0394.

We compare the performance of our PCGS method with that of the SAGE method [7]. Note that the latter uses the true $\mathbf{h}$ and the true number of dominant MPCs as prior knowledge, whereas these quantities are estimated by our method. For each realization of $\mathbf{y}$, our method generates a Markov chain by means of the PCGS. Simulations have shown that, due to fast convergence, a chain of length 10 is sufficient. The last $I=7$ realizations were used for detection/estimation. To quantify the overall deviation of the $\hat{L}$ detected time-angle locations $\{(\hat{k}_i,\hat{q}_i)\}_{i=1}^{\hat{L}}$ in $\hat{\hat{\boldsymbol{\alpha}}}$ from the L_{dom} true locations $\{(k_j,q_j)\}_{j=1}^{L_{\text{dom}}}$ in $\boldsymbol{\alpha}_{\text{dom}}$, we use a "distance" ϵ defined as $\min_{i=1,\ldots,\hat{L}}\sqrt{(\hat{k}_i-k_j)^2+(\hat{q}_i-q_j)^2}$, averaged over the L_{dom} true locations (i.e., $j=1,\ldots,L_{\text{dom}}$) and over 100 realizations, and multiplied by the correction factor $\hat{L}/L_{\text{dom}}$. Note that, trivially, $\hat{L}=L_{\text{dom}}$ for the SAGE method. Fig. 1 shows ϵ versus β. Our method is clearly more accurate than the SAGE method; however, the processing time is longer by a factor of about 50.

Fig. 2 shows the results of the two methods for a real UWB signal, which was obtained from measurements described in [7]. It is seen that our method detects dominant MPCs that are not detected by the SAGE method, and it avoids double detection.

6. CONCLUSION

We proposed a partially collapsed Gibbs sampler method for determining the parameters of multipath components (MPCs) of UWB channels from signals received by a 2D antenna array. Our method jointly estimates the number, times-of-arrival, angles-of-arrival, and amplitudes of MPCs as well as the sounding pulse. The detection of spurious MPCs is avoided by using a combined detection/estimation approach (with detection of MPC indicators) and a temporal-angular minimum distance constraint. The signal delay between different antennas—which is relevant due to the shortness of UWB pulses—is taken into account by our signal model. The proposed method was successfully applied to synthetic and real UWB signals.

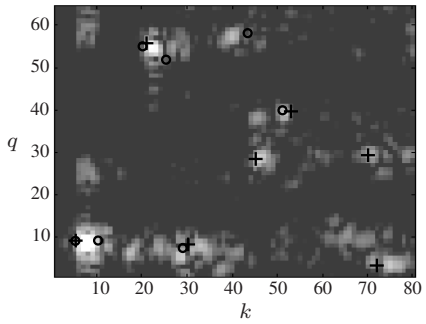

Fig. 2. Magnitude of the direction-resolved received signal $z[k,q]\triangleq\sum_{m=1}^{M}c_m^*[q]\,y_m[k]$ for a real UWB signal (line-of-sight scenario [7]), with the time-angle locations of the detected MPCs marked by "+" (proposed PCGS method) and "o" (SAGE method [7]).

7. ACKNOWLEDGMENT

The authors would like to thank K. Hausmair for providing the SAGE code used in Section 5.

8. REFERENCES

[1] Y. Shen and M. Win, "On the use of multipath geometry for wideband cooperative localization," in *Proc. IEEE GLOBECOM 2009*, Honolulu, HI, Nov.–Dec. 2009.

[2] P. Meissner, T. Gigl, and K. Witrisal, "UWB sequential Monte Carlo positioning using virtual anchors," in *Proc. Int. Conf. Indoor Posit. Indoor Navig. (IPIN)*, Zurich, Switzerland, Sep. 2010.

[3] R. J.-M. Cramer, R. A. Scholtz, and M. Win, "Evaluation of an ultra-wide-band propagation channel," *IEEE Trans. Antenn. Propag.*, vol. 50, pp. 561–570, May 2002.

[4] T. Santos, J. Karedal, P. Almers, F. Tufvesson, and A. F. Molisch, "Modeling the ultra-wideband outdoor channel: Measurements and parameter extraction method," *IEEE Trans. Wireless Comm.*, vol. 9, pp. 282–290, Jan. 2010.

[5] K. Haneda and J.-I. Takada, "An application of SAGE algorithm for UWB propagation channel estimation," in *Proc. 2003 IEEE Conf. UWB Syst. Technol.*, Reston, VA, pp. 483–487, Nov. 2003.

[6] B. Fleury, D. Dahlhaus, R. Heddergott, and M. Tschudin, "Wideband angle of arrival estimation using the SAGE algorithm," in *Proc. IEEE 4th Int. Sympos. Spread Spectr. Techn. Applic. Proc.*, vol. 1, Mainz, Germany, pp. 79–84, Sep. 1996.

[7] K. Hausmair, K. Witrisal, P. Meissner, C. Steiner, and G. Kail, "SAGE algorithm for UWB channel parameter estimation," in *Proc. COST 2100 Management Committee Meeting*, Athens, Greece, Feb. 2010.

[8] D. A. van Dyk and T. Park, "Partially collapsed Gibbs samplers: Theory and methods," *J. Am. Statist. Assoc.*, vol. 103, pp. 790–796, June 2008.

[9] G. Kail, J.-Y. Tourneret, F. Hlawatsch, and N. Dobigeon, "A partially collapsed Gibbs sampler for parameters with local constraints," in *Proc. IEEE ICASSP-2010*, Dallas, TX, pp. 3886–3889, March 2010.

[10] C. P. Robert and G. Casella, *Monte Carlo Statistical Methods*. New York, NY: Springer, 2004.

[11] D. Ge, J. Idier, and E. Le Carpentier, "Enhanced sampling schemes for MCMC based blind Bernoulli-Gaussian deconvolution," *Signal Processing*, vol. 91, pp. 759–772, Apr. 2011.

[12] G. Kail, F. Hlawatsch, and C. Novak, "Efficient Bayesian detection of multiple events with a minimum-distance constraint," in *Proc. IEEE SSP-09*, Cardiff, Wales, UK, pp. 73–76, Aug.–Sep. 2009.